# Generalized Plane Piezoelectric Problem: Application to Heterostructure Nanowires

H. T. Mengistu and A. Garcia-Cristobal
*Institute of Material Science, University of Valencia, P.O.Box 22085, E-46071, Valencia, Spain*
**Heruy.Mengistu@uv.es*

**Abstract:** In this work we first present a general theoretical framework for the two-dimensional (2D) modeling of piezoelectric problems in translationally invariant three-dimensional (3D) systems. This 2D approach is called here the Generalized Plane Piezoelectric (GPP) problem. Then, a computational methodology is developed and implemented on the COMSOL Multiphysics software platform. Finally, as an application of the developed approach, we study the piezoelectric response in lattice-mismatched heterostructure (core-shell) nanowires.

**Keywords:** Piezoelectricity, Finite Element Method, Generalized Plane Piezoelectric Problem, Nanowires.

## 1. Introduction

In order to analyze the piezoelectric behavior of materials, it is necessary to solve the coupled mechanical and electrical equations of piezo-electricity. However, the numerical simulations of discretized electro-mechanical equations for 3D systems are in general computationally expensive. Therefore, the disposal of two-dimensional (2D) approaches to problems originally posed in a 3D geometry is always desirable, since they significantly reduce the computing resources and simulation time needed.

The simplest approach for approximating 3D piezoelectric problems into a mathematically 2D framework relies on the assumption that the displacement and electric field components ($u_3$ and $E_3$) along $X_3(\equiv Z)$ axis vanish, and that the remaining components depend only on in-plane coordinates, $(x_1, x_2)$(standard Plane Approximation) [1]. However, there are many problems where the piezoelectric medium develops out-of-plane axial ($\varepsilon_{33}$) and shear ($\varepsilon_{13}$ and $\varepsilon_{23}$) strain components and/or axial electric field component. ($E_3$) that cannot be captured by the above 2D approach.

In Sec. 2 we report on a more general 2D approach, based on the idea that for (indefinite) systems with geometry, material properties and boundary conditions independent of the coordinate $x_3(\equiv z)$, the strain and electric field components ($\varepsilon_{ij}$ and $E_i$) depend only on the in-plane coordinates, $(x_1, x_2)$. Under this sole hypothesis, the original 3D problem can be reformulated into a 2D mathematical framework called here the Generalized Plane Piezoelectric (GPP) problem [2]. The GPP problem is expected to be a good approximation for finite but long 3D wire-like systems, where the deformation and electric field are mostly uniform along the $x_3$ axis (except possibly near the end surfaces).

In order to perform numerical calculations based on the GPP approach, an attractive option is to use the finite element method, as implemented, for instance, in the COMSOL Multiphysics software platform. In Sec. 3 we give details of how to arrange the GPP problem in a way that can be easily implemented within the COMSOL software.

Finally, the above procedure is illustrated in Sec. 4 by calculating the electric fields and piezoelectric potential in a free-standing lattice-mismatched core-shell nanowire.

## 2. The Generalized Plane piezoelectric Problem

We start with a summary of the general formulations of 3D linear piezoelectric problem in a domain *D*. Cartesian index notation ($i, j, k, l = 1,2,3$ and $\alpha, \beta = 1,2$) and Einstein summation convention for repeated indices are used throughout the paper.

The strain tensor $\varepsilon_{ij}$ and the electric field $E_i$ are related to the mechanical displacement $u_i$ and the electric potential $\phi$ through the relations:

$$\varepsilon_{ij} = \frac{1}{2}\left(\frac{\partial u_i}{\partial x_j} + \frac{\partial u_j}{\partial x_i}\right), \quad (1a)$$

$$E_i = -\frac{\partial \phi}{\partial x_i}\ . \quad (1b)$$

The equilibrium equations are given by Navier and Poisson equations as:

$$\frac{\partial \sigma_{ij}}{\partial x_j} = -f_i\ , \quad (2a)$$

$$\frac{\partial D_i}{\partial x_i} = \rho\ , \quad (2b)$$

where $\sigma_{ij}$ is the stress tensor and $D_j$ is the dielectric displacement vector. The right-hand terms are given by the body force $f_i$ and the volumic charge density $\rho$.

The linear fully-coupled constitutive relations for mechanical stress and electric displacement are given as [3]:

$$\sigma_{ij} = C_{ijkl}\varepsilon_{kl} - e_{kij}E_k\ , \quad (3a)$$

$$D_i = e_{ikl}\varepsilon_{kl} + \in_{ij} E_k\ , \quad (3b)$$

or, schematically,

$$\sigma = C:\varepsilon - e:E\ ,$$

$$D = e:\varepsilon + \in:E\ ,$$

where $C_{ijkl}$ are the elastic constants, $e_{kij}$ are the piezoelectric constants and $\in_{ij}$ are the dielectric tensor components.

It can be shown that the particular problem of heterogeneous lattice-mismatched body containing regions with different material constants [ $C_{ijkl}(r)$ , $e_{kij}(r)$ , $\in_{ij}(r)$ ] and lattice parameters [ $a_k(r)$ ] can be mapped to a standard piezoelectric problem by the introduction of equivalent body force $f_i^{(0)}$ and charge density $\rho^{(0)}$:

$$f_i^{(0)} = \frac{\partial}{\partial x_j}\left[\, C_{ijkl}(r)\varepsilon_{kl}^{(0)}(r)\right],$$

$$\rho^{(0)} = -\frac{\partial}{\partial x_i}\left[e_{ikl}(r)\varepsilon_{kl}^{(0)}(r)\right].$$

The lattice mismatch (*misfit*) strain $\varepsilon_{kl}^{(0)}(r)$ is given as:

$$\varepsilon_{kl}^{(0)}(r) = \frac{a_k^{(\mathrm{ref})} - a_k(r)}{a_k(r)}\ \delta_{kl}\ ,$$

where $a_k^{(\mathrm{ref})}$ are the parameters of a convenient lattice reference. In this case, the total deformation with respect to the local lattice is given by $\varepsilon_{kl}^{(T)}(r) = \varepsilon_{kl}^{(0)}(r) + \varepsilon_{kl}(r)$.

The equations (1), (2) and (3), supplemented with appropriate boundary conditions constitute the complete mathematical definition of a 3D linear fully-coupled piezoelectric problem.

Direct simulations of 3D problems require large computing resources. However, as we have proven in a previous work on the purely elastic problem [4], if certain additional conditions are required, the above framework can be cast into a mathematically 2D problem. Those conditions are as follows: Let us assume that we have a system, indefinite along one longitudinal direction (taken to be the $x_3 \equiv z$ axis), whose transverse geometrical description (i.e., cross-section), material properties, loads, and eventual boundary or interface conditions are independent of the $x_3$ coordinate. For such a system all the cross sections along the longitudinal axis can be considered to be at identical conditions and, therefore, one can make the ansatz [2]:

$$\varepsilon_{ij} = \varepsilon_{ij}(x_1, x_2)\ , \quad (4a)$$

$$E_k = E_k(x_1, x_2)\ . \quad (4b)$$

By using Eq. (4) together with Eq. (1) the displacement and electric fields are shown to have the following structure [5]:

$$\begin{aligned} u_1 &= U_1(x_1, x_2) - \frac{A}{2}{x_3}^2 + \Theta\, x_2 x_3\ , \\ u_2 &= U_2(x_1, x_2) - \frac{B}{2}{x_3}^2 - \Theta\, x_1 x_3\ , \\ u_3 &= U_3(x_1, x_2) + (Ax_1 + Bx_2 + C)x_3\ . \end{aligned} \quad (5a)$$

$$\phi = \Phi(x_1, x_2) + E_0\, x_3\ . \quad (5b)$$

The corresponding strain can then be written as:

$$\varepsilon_{ij} = \varepsilon_{ij}^{(U)} + \varepsilon_{ij}^{(\bullet)}\ , \quad (6a)$$

where

$$\varepsilon_{ij}^{(U)} \leftrightarrow \begin{pmatrix} \dfrac{\partial U_1}{\partial x_1} & \dfrac{1}{2}\left(\dfrac{\partial U_1}{\partial x_2} + \dfrac{\partial U_2}{\partial x_1}\right) & \dfrac{1}{2}\dfrac{\partial U_3}{\partial x_1} \\ sym. & \dfrac{\partial U_2}{\partial x_2} & \dfrac{1}{2}\dfrac{\partial U_3}{\partial x_2} \\ sym. & sym. & 0 \end{pmatrix},$$

$$\varepsilon_{ij}^{(\bullet)} \leftrightarrow \begin{pmatrix} 0 & 0 & \dfrac{1}{2}\Theta\, x_2 \\ sym. & 0 & -\dfrac{1}{2}\Theta\, x_1 \\ sym. & sym. & Ax_1 + Bx_2 + C \end{pmatrix},$$

and the electric field is:

$$E = \begin{pmatrix} -\dfrac{\partial \Phi}{\partial x_1} \\ -\dfrac{\partial \Phi}{\partial x_2} \\ 0 \end{pmatrix} + \begin{pmatrix} 0 \\ 0 \\ E_0 \end{pmatrix} \equiv E^{(\Phi)} + E^{(\bullet)}\ . \quad (6b)$$

and the equilibrium equations (2) become:

$$\frac{\partial}{\partial x_\alpha}[\sigma_{i\alpha}^{(U)} + \sigma_{i\alpha}^{(\bullet)}] = -f_i\ , \quad (7a)$$

$$\frac{\partial}{\partial x_\alpha}[D_i^{(\Phi)} + D_i^{(\bullet)}] = \rho\ . \quad (7b)$$

Here, $U_i$ and $\Phi$ are the mathematically 2D (i.e., dependent only on $(x_1, x_2)$ ) displacement and potential, $C$ is the axial strain, $A$ and $B$ are bending strains, $\Theta$ characterizes the torsion of the system, and $E_0$ is the axial electric field.

The above equations must be supplemented with conditions on the boundary limiting the cross section of the body, and boundary conditions at the far end surfaces $S_{\pm}$ (at $x_3 \to \pm\infty$). These latter conditions are usually required not pointwise but in an integrated sense, e.g, by specifying the total force and torque [1]:

$$F = \int_{S_+} t\, dS \quad \text{and} \quad M = \int_{S_+} r \times t\, dS\ , \qquad (8a)$$

$$Q = \int_{S_+} D_3 dS\ , \qquad (8b)$$

where $t_i = \sigma_{i3}$ are the components of the traction vector field at $S_+$.

The set of equations (5)-(7), together with boundary conditions (8) define a 2D problem where the fields $U_i(x_1, x_2)$ and $\Phi(x_1, x_2)$, and the constants $(A, B, C, \Theta, E_0)$, have to be determined. This problem is called here the Generalized Plane Piezoelectric (GPP) problem. We note that the GPP approach is able to accommodate any cross section geometry and elastic symmetry, and a wide range of compatible boundary conditions, corresponding to different kinds of externally applied stresses (such as hydrostatic pressure, bending moments...) and charges.

The GPP problem refers of course to an idealized situation but, according to the Saint Venant principle, it is supposed to be a good approximation for 3D finite but long system fulfilling the translational invariance conditions mentioned above. The quality of this approximation is illustrated by the numerical simulations in Sec.4.

## 3. COMSOL Multiphysics implementation

The numerical calculations of GPP problem are done by using finite element method as implemented in the piezoelectric module of the COMSOL Multiphysics software platform [6]. In this module the piezoelectric equilibrium conditions are implemented via the virtual work principle, leading to a weak formulation of Eq. (2), which can be written schematically as[7]:

$$\int_D u_{test} \cdot (\nabla . \sigma + f) = 0, \qquad (9a)$$

$$\int_D \phi_{test} (\nabla . D - \rho) = 0 \qquad (9b)$$

Where $u_{test}$ and $\phi_{test}$ are the test functions for the displacement fields and piezoelectric potential respectively.

The Piezoelectric Mechanics module allows to use the standard Plane Strain based piezoelectric approximation within the Plane Strain application mode[7]. However, the antiplane displacement variable $U_3$ , the strain $\varepsilon_{ij}^{(\bullet)}$ and the out-of-plane electric field $E^{(\bullet)}$ are not available or easily implementable in the Plane Strain application mode, so it is not useful to make computations of the GPP problem.

We have instead implemented the GPP problem within the Piezoelectric module of COMSOL by means of the following procedure. First, we note that, by using Eq. (6), the weak condition (9) becomes:

$$\int_D \left(-\sigma^{(U)} \cdot \varepsilon_{test}^{(U)} + f \cdot U_{test}\right) + \text{surf. term1} + \int_D \left(-\sigma^{(\bullet)} \cdot \varepsilon_{test}^{(U)} - \sigma \cdot \varepsilon_{test}^{(\bullet)}\right) = 0 \qquad (10a)$$

$$\int_D \left(D^{(\phi)} \cdot E_{test}^{(\phi)} + \rho \cdot \Phi_{test}\right) + \text{surf. term2} + \int_D \left(D^{(\phi)} \cdot E^{(\Phi)}{}_{test} + D \cdot E_{test}^{(\bullet)}\right) = 0 \qquad (10b)$$

The terms in the first line of Eq. (10a) and Eq. (10b) correspond to the "partial" piezoelectric problem associated to displacement $U_i(x_1, x_2)$ and piezoelectric potential $\phi\,(x_1, x_2)$. This problem can be solved by using the 3D application mode on a finite length slice of the original infinitely extended system. The cross section is conveniently meshed. In order to force the dependence on $(x_1, x_2)$ we use the following trick: We mesh the length of the slice with only one quadrilateral element (what simply doubles the total number of elements used to mesh the cross section) and require periodic boundary conditions to connect the top and bottom surfaces of the slice. This trick effectively imposes that the numerical solutions, that is to be interpreted as $U_i$ and $\phi$, do not depend on $x_3$.

However, it still remains to incorporate the contribution of $\varepsilon^{(\bullet)}$ and $E^{(\bullet)}$ to the weak condition (10). This is implemented as follows: Since $(A, B, C, \Theta, E_0)$ can be considered as additional degrees of freedom that are constant throughout the modeled cross section, it is convenient to include them in the COMSOL

program as extra unknown global variables [8]. Then, the contributions containing those variables in the second line of Eq. (10a) and Eq. (10b) are added as weak terms to the 3D problem related to $U_i$ and $\phi$ by means of the "Weak Contribution" feature of COMSOL [8].

The boundary conditions Eq.(8) can eventually be implemented by making use of the "Weak Constraint" feature of COMSOL [8].

The solution of the 3D application mode modified as explained above gives the desired results for $U_i(x_1, x_2)$, $\phi(x_1, x_2)$ and constants $(A, B, C, \Theta, E_0)$.

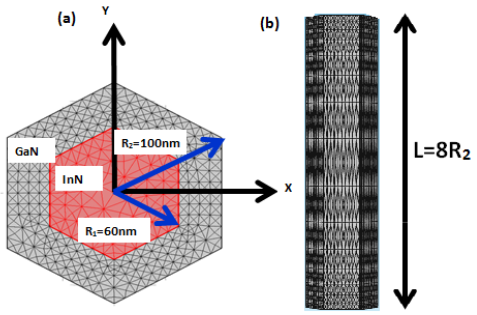


**Figure 1**. Geometry of the Hexagonal InN/GaN core-shell nanowires investigated with details about the meshes employed with radius of core $R_1$=60nm and Radius of shell $R_2$=100nm.

**Table-1** Parameters used in the numerical calculation.

| | InN | GaN |
|---|---|---|
| Lattice parameter | | |
| $a_0$ (Å) | 4.98 | 4.50 |
| Elastic constants | | |
| $C_{11}$(GPa) | 204.1 | 316.9 |
| $C_{12}$(GPa) | 119.4 | 152.0 |
| $C_{44}$(GPa) | 114.1 | 197.6 |
| Piezoelectric constants (C/$m^2$) | | |
| $e_{14}$ | 0.84 | 0.59 |
| Relative permittivity ( $\in_0$) | | |
| $\in_r$ | 8.4 | 9.7 |

## 4. Numerical Results

In order to illustrate the GPP problem and its implementation in COMSOL we have performed numerical calculations of the electric field and piezoelectric potential distributions in an infinite hexagonal core-shell nanowire. The core is made of InN and the shell is made of GaN. Both materials exhibit cubic elastic symmetry and their longitudinal axes coincide with the [111] crystallographic direction. In Fig. 1(a) we display the cross section mesh used for the GPP problem. The X- and Y-axes are taken along $[\bar{1}10]$ and $[11\bar{2}]$ crystallographic directions, respectively. We assume that the nanowire is free from external tractions, body forces and charge, so that the strain and electric field are solely induced by the internal lattice-mismatch body force $f_i^{(0)}$ and charge $\rho^{(0)}$. Material parameters used can be found in Table I. In order to test the quality of our GPP approach, we have also performed standard 3D calculations for a finite but long nanowire. The longitudinal mesh employed is displayed in Fig. 1 (b).

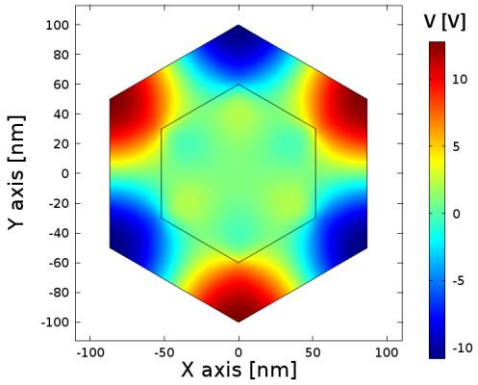


**Figure 2**. Piezoelectric potential $\phi(x_1, x_2)$ obtained by GPP problem approach.

Figure-2 shows details of the piezoelectric potential distribution throughout the nanowire cross section, as obtained within the GPP approach. The highest value of piezoelectric potential developed is localized inside the shell GaN and corresponds to maximum in-plane potential of $\phi_{max}$=11.78V while the core InN is highly dominated by zero potential.

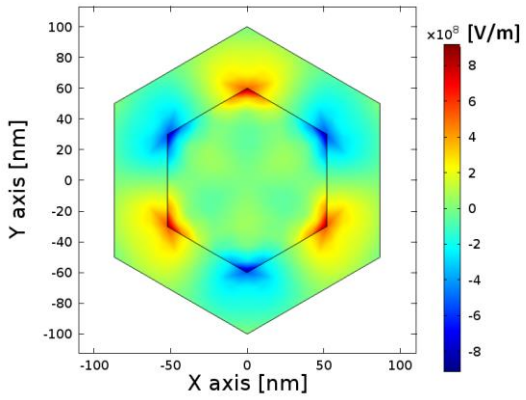


**Figure 3**. Electric field in the radial direction $E_r(x_1, x_2)$ obtained by GPP problem approach.

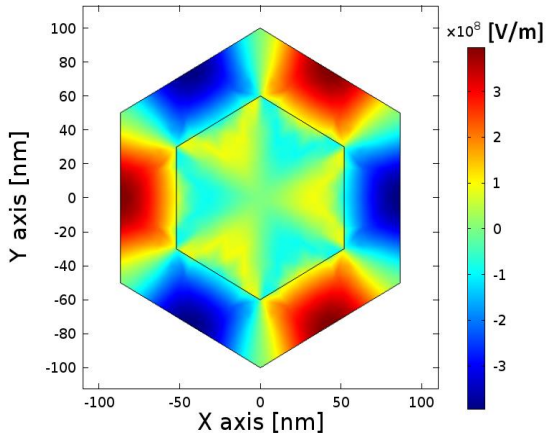


**Figure 4**. Electric field in the angular direction $E_\phi(x_1, x_2)$ obtained by GPP problem approach.

Figures 3 and 4 show details of the electric field (cylindrical) components in the radial and angular ($E_r(x_1, x_2)$, and $E_\phi(x_1, x_2)$) directions throughout the nanowire cross section respectively as obtained within the GPP problem approach. In the radial direction the maximum in-plane electric field corresponds to $E_{r\,max}$=925.14 MV/m and is confined at the corners of the core-shell interface. On the other hand, the electric field in the angular direction corresponds to maximum in-plane electric field of $E_{\phi\,max}$= 397.42 MV/m and is localized inside the shell. The electric field in the axial direction corresponds to $E_0$= 136.14 MV/m pointing in the same direction as the in-plane electric fields.

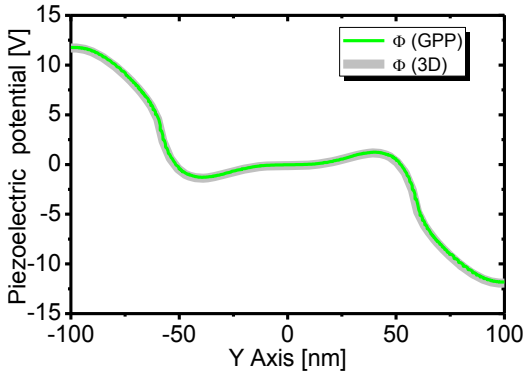


**Figure 5**. Y-axis linescan comparison of piezoelectric potential $\phi(x_1, x_2)$ obtained by GPP problem and the direct 3D approaches.

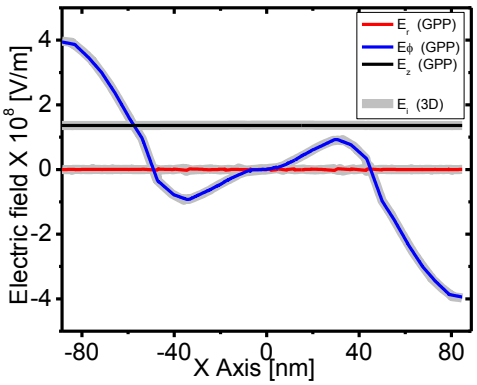


**Figure 6**. X-axis line scan comparison of the Electric field components obtained by GPP approach and the direct 3D approaches.

In Fig. 5 and Fig. 6 we present Y-axis linescan comparisons of piezoelectric potential ($\phi$) and X-axis linescans of the Electric field (cylindrical) components ($E_r$, $E_\phi$, and $E_z$) corresponding to the GPP problem and to the central cross section of the finite 3D problem. We see that the agreement between the piezoelectric potential and electric field profiles of both approaches is excellent virtually indistinguishable in the figure thus showing the reliability of the GPP approach to simulate the central region of large aspect-ratio piezoelectric problems.

## 5. Conclusions

In this paper we have presented a theoretical framework called Generalized Plane piezoelectric problem (GPP) and implemented a computational methodology within the COMSOL Multiphysics software platform that allows efficient and inexpensive numerical calculations of the strain distribution in a wide class of translationally invariant systems. We have performed model simulations in a core-shell nanowire that show an excellent agreement when compared with direct 3D calculations for a long nanowire. This agreement shows the reliability of the GPP approach to obtain efficiently accurate strain distributions for wire-like systems.

## 6. References


1. Chyanbin Hwu Anisotropic Elastic Plates, (*Springer , New York*; 2010.
2. S. G Lekhnitskii, *Theory of elasticity of an anisotropic elastic body* (San Francisco: Holden-Day, San Francisco, 1963).
3. A. H. Meitzler, H. F. Tiersten, A. W. Warner, D. Berlincourt, G. A. Couqin and F. S. Welsh, III, *IEEE Standard on Piezoelectricity*, IEEE, New York, 1988 .
4. H. T. Mengistu and A. Garcia-Cristobal, Generalized Plane Strain Problem: Application to Heterostructure Nanowires**,** *COMSOL User Conference*, Malaga, Spain, (2014).
5. Tungyang Chen and Donsen Lai, An exact correspondence between plane piezoelectricity and generalized plane strain in elasticity, *Proc. R. Soc. Lond. A* ***453,*** 2689 2713 (1997).
6. http://www.comsol.com/comsol-multiphysics
7. See the *Structural Mechanics Module User's Guide* for more details.
8. See the *COMSOL Multiphysics User's Guide* for more details.


## 7. Acknowledgement


This work has been financially supported by the European Union through the Grant Agreement No.265073-NANOWIRING of the Seventh Framework Program, and by the Ministry of Finances and Competitiveness (MINECO) of Spain through Grants CSD2010-00044 of the Programme ''Consolider Ingenio 2010'' and MAT2012-33483.


## 8. Appendix

### Appendix A. Elasticity matrix

The elasticity matrix of materials with zincblende structure in [001] crystallographic direction is given as:

$$C^{ZB}_{[001]} = \begin{pmatrix} C_{11} & C_{12} & C_{12} & 0 & 0 & 0 \\ C_{12} & C_{11} & C_{12} & 0 & 0 & 0 \\ C_{12} & C_{12} & C_{11} & 0 & 0 & 0 \\ 0 & 0 & 0 & C_{44} & 0 & 0 \\ 0 & 0 & 0 & 0 & C_{44} & 0 \\ 0 & 0 & 0 & 0 & 0 & C_{44} \end{pmatrix}$$

In [111] crystallographic direction it takes the form:

$$C^{ZB}_{[111]} = \begin{pmatrix} C^z_{11} & C^z_{12} & C^z_{12} & C^z_{14} & 0 & 0 \\ C^z_{12} & C^z_{11} & C^z_{12} & -C^z_{14} & 0 & 0 \\ C^z_{12} & C^z_{12} & C^z_{33} & 0 & 0 & 0 \\ C^z_{14} & -C^z_{14} & 0 & C^z_{44} & 0 & 0 \\ 0 & 0 & 0 & 0 & C^z_{44} & C^z_{14} \\ 0 & 0 & 0 & 0 & C^z_{14} & C^z_{66} \end{pmatrix}$$

Where,

$$C^z_{11}=(C_{11}+C_{12}+2C_{44})/2$$
$$C^z_{12}=(C_{11}+5C_{12}-2C_{44})/6$$
$$C^z_{13}=(C_{11}+2C_{12}-2C_{44})/3$$
$$C^z_{14}=(-C_{11}+C_{12}+2C_{44})\sqrt{2}/6$$
$$C^z_{33}=(C_{11}+2C_{12}+4C_{44})/3$$
$$C^z_{44}=(C_{11}-C_{12}+C_{44})/3$$
$$C^z_{66}=(C_{11}-C_{12}+4C_{44})/6$$

### Appendix B. Piezoelectric coupling matrix

The piezoelectric coupling matrix for zincblende structure in [001] crystallographic direction becomes:

$$e^{ZB}_{[001]} = \begin{pmatrix} 0 & 0 & 0 & e_{14} & 0 & 0 \\ 0 & 0 & 0 & 0 & e_{14} & 0 \\ 0 & 0 & 0 & 0 & 0 & e_{14} \end{pmatrix}^T$$

In [111] crystallographic directions it takes the form:

$$e^{ZB}_{[111]} = \begin{pmatrix} 0 & 0 & 0 & 0 & -e^z_{14} & -\sqrt{2}e^z_{14} \\ -\sqrt{2}e^z_{14} & \sqrt{2}e^z_{14} & 0 & -e^z_{14} & 0 & 0 \\ -e^z_{14} & -e^z_{14} & 2e^z_{14} & 0 & 0 & 0 \end{pmatrix}^T$$

Where $e^z_{14}=e_{14}/\sqrt{3}$.